

Gas Identification Using Passive UHF RFID Sensor Platform

^{1,*} Muhammad Ali AKBAR, ² Mohamed ZGAREN, ¹ Amine AIT SI ALI,
¹ Abbes AMIRA, ¹ Mohieddine BENAMMAR, ¹ Faycal BENSALI,
² Mohamad SAWAN and ³ Amine BERMAK

¹ College of Engineering, Qatar University, Doha, Qatar

² Dept. of Electrical Engineering, Polytechnique Montreal, Montreal, Quebec, Canada

³ School of Engineering, Hong Kong Uni. of Sci. and Tech., Clear Water Bay, Hong Kong

* E-mail: ali.akbar@qu.edu.qa

Received: 31 August 2015 / Accepted: 15 October 2015 / Published: 30 November 2015

Abstract: The concept of passive Radio Frequency Identification (RFID) sensor tag is introduced to remove the dependency of current RFID platforms on battery life. In this paper, a gas identification system is presented using passive RFID sensor tag along with the processing unit. The RFID system is compliant to Electronics Product Code Generation 2 (EPC-Gen2) protocol in 902-928 MHz ISM band. Whereas the processing unit is implemented and analyzed in software and hardware platforms. The software platform uses MATLAB, whereas a High Level Synthesis (HLS) tool is used to implement the processing unit on a Zynq platform. Moreover, two sets of different gases are used along with Principal Component Analysis (PCA) and Linear Discriminant Analysis (LDA) based feature reduction approaches to analyze in detail the best feature reduction approach for efficient classification of gas data. It is found that for the first set of gases, 90 % gases are identified using first three principal components, which is 7 % more efficient than LDA. However in terms of hardware overhead, LDA requires 50 % less hardware resources than PCA. The classification results for the second set of gases reveal that 91 % of gas classification is obtained using LDA and first four PCA, while LDA requires 52 % less hardware resources than PCA. The RFID tag used for transmission is implemented in 0.13 μm CMOS process, with simulated average power consumption of 2.6 μW from 1.2 V supply. ThingMagic M6e embedded reader is used for RFID platform implementation. It shows an output power of 31.5 dBm which allows a read range up to 9 meters. *Copyright* © 2015 IFSA Publishing, S. L.

Keywords: Sensor tag, Pattern recognition, Gas identification, UHF RFID Reader, EPC Gen2, ISM Band.

1. Introduction

Gas identification is one of the most critical challenges in the current gas industry because a single leakage of an explosive gas can cause a complete disaster for the whole company. The explosion of a gas container or the leakage of a hazardous gas will also be disastrous for the environment [1]. Therefore,

human olfactory based Electronic Nose (EN) systems are introduced, with a wide range of applications like milk industry [2] and patient monitoring system [3].

In gas applications, the presence of complex compounds like water vapor with the gases of interest creates one of the challenging issues for the gas identification using EN [4]. The presence of battery further limits the life and durability of the sensor tag.

Moreover, the drift and non-selectivity of sensor raise the problem of classification for EN [5]. The possible approaches to deal with the problem of drift and non-selectivity is to increase the number of sensors as adopted by Guo, *et al.* [6] Guo to introduce the temperature modulation such that a single sensor provides the different responses for the same gas due to temperature variations [7]. The purpose of these approaches is to get more signatures for the same gas, whereas both approaches of multiple-sensors and single sensor-modulation increase the dimensionality of feature vectors, thereby increasing the computational complexity. The problem becomes more severe if the gas identification system is implemented on any hardware platform because of resource utilization and power consumption which increases with the computational complexity. Therefore, to feature reduction approaches like Principal Component Analysis (PCA) or Linear Discriminant Analysis (LDA) is required to reduce the data size and increase the processing efficiency. On the other hand, Radio Frequency Identification (RFID) sensing design has been widely explored as a low-cost candidate toward lightweight, reliable and energy-efficient devices for gas detection [8]. There has been a permanent evolution toward combining the capabilities of gas sensing and wireless technology in order to collect, process, and transmit time-varying data. This approach leads to RFID-enabled Wireless Sensor Network (WSN) infrastructure. Most of the WSN includes a battery [9], which increases their cost and limits their autonomy. The power autonomy can be encountered by using a fully passive (battery-less) UHF RFID design. A typical RFID system is mainly composed of a reader and antenna (also named interrogator), one to several tags (also named electronic labels) and an information systems back-end.

Furthermore, a reconfigurable hardware is required to improve the processing time for run-time classification because a dedicated hardware is faster than the software application. However, gas recognition process requires a complicated training phase and frequent calibration, which is even harder to implement on a dedicated hardware. As a consequence, most EN solutions nowadays are software-based platforms and the integration of a real-time in-site training and portable EN microsystem is yet to be demonstrated. Therefore, a hardware-based processing unit is demonstrated which can be applied in any multi-sensing gas identification platform. The presence of a processor along with programmable logic blocks based on field programmable gate array (FPGA) has made the heterogeneous Zynq platform suitable for our research. A hybrid system can easily be implemented on Zynq using High Level Synthesis (HLS) tool. The other reason for using Zynq board is because the circuit implemented and tested on it can be reproduced to application-specific integrated circuit (ASIC).

Therefore, in this paper the reader of a passive Ultra-High Frequency (UHF) RFID sensor platform is

presented with a centralized hardware processing unit to perform feature reduction and classification. The data from multiple sensor tags will be collected using M6e embedded reader at the central processing unit with respect to the Electronic Product Code Generation 2 (EPC-Gen2) protocol in the 902-928 MHz ISM frequency band. Each sensor tag has a 4×4 array gas sensor proposed by Guo, *et al.* [6] and a low power, temperature sensor [10]. Moreover, a unique code is associated with all sensor tags individually, which helps the processing unit to identify the tag and process the collected data accordingly. The central processing unit is tested on a heterogeneous reconfigurable Zynq platform using High-Level Synthesis (HLS) tools while the tag sensors are implemented in CMOS process to reduce the power dissipation and enhance the full system integration. The presented work is part of an ongoing project in which a low-power multi-sensing gas identification platform is needed to be developed for gas identification based on an array of tin-oxide gas sensors.

The remaining parts of this paper are organized as follows. Section 2 and 3 cover the RFID sensor tag along with the experimental setup for data acquisition. The UHF RFID tags is described in Section 4. Section 5 is concerned with the processing unit. Simulation results are shown and discussed in Section 6. Section 7 concludes the paper.

2. RFID Sensor Platform and Data Extraction

The UHF RFID based sensor platform includes a 4×4 array gas sensor [6] and a low power temperature sensor [10]. The main challenge of the RFID sensor design is the power hungry, building blocks for which an external power source is required. Whereas, the presence of battery in the sensor tag limits the lifetime of the tag-based sensors. Tags will not be able to communicate with the embedded reader if battery power level goes below a fixed threshold. Therefore, a fully passive UHF RFID approach is adopted such that, the communication link between tags based sensor and the reader is guaranteed for longer time. The full tags based sensor system are powered by a remote power through the RF energy received from the reader in order to create autonomous gas measurement microsystems.

The main challenge with the passive RFID tag is the limited range of communication; therefore, hybrid design could be used by adding a battery as power bank in addition to harvesting the power circuit. The power bank will allow to reach higher communication ranges when needed.

In order to test the sensor tag, data is extracted for two different sets of gases. The first set of gases (GS1) included Carbon-mono-oxide, ethanol and hydrogen in which 10 concentrations of each gas are used in a fixed laboratory environment, i.e. 20, 40, 60, 80, 100,

120, 140, 160, 180 and 200 ppm in air. However, since a tin-oxide base gas sensor is used which is dependent on the operating temperature, therefore the data acquired for a second set of gases (GS2) with 4 concentrations of each C₆H₆, CH₂O, CO, NO₂ and SO₂, on three operating temperatures i.e. 200, 300 and 400°C. The sensor values obtained at three different temperatures are then merged to define the training and testing data for the second set.

The extraction process of gas data is carried out in an identical way in both cases that the dry air is flushed for 750 s before exposing the sensor to any new

concentration of gas. The sensor is then exposed to the gas in a closed glass chamber for 250 s and 750 s respectively, for GS1 and GS2. This is due to the fact that the sensor reaches steady state after 250 s for GS1 and it takes 750 s to obtain steady state for GS2. The experiment is repeated again after obtaining the data for given concentrations of each gas such that the obtained data is divided into two parts. The first one is used for training purpose known as learning data (DI) and the second one for testing purpose known as test data (Dt). The overall model of sensor tag is shown in Fig. 1.

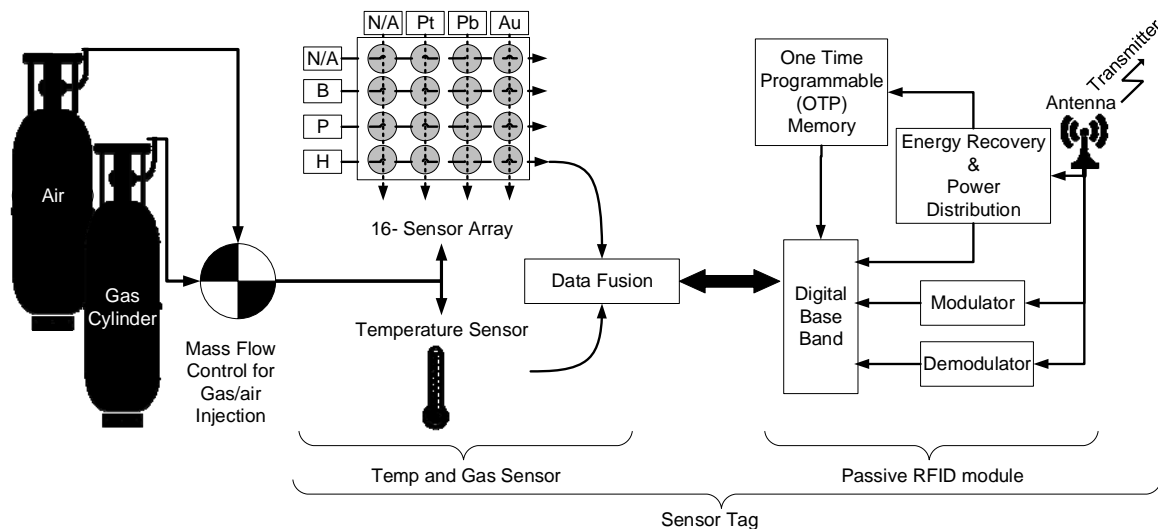


Fig. 1. Block Diagram of RFID Sensor tag with data acquisition setup.

3. UHF RFID Reader Performance

A typical RFID system consists of tags, readers and computer application systems, as shown in Fig. 2. With several excellent characteristics, such as portable, high capacity, long life, security access, and movable recognition, RFID are used more and more widely in logistics, production management, and monitoring and tracking applications [11]. The EPC Gen2 protocol was designed based on the minimal features available on an EPC Gen2 RFID tag specifically a 32-bit secret access password, a 16-bit pseudo-random number generator, and limited memory that can store at least two 16-bit random numbers while the tag is powered. An improved authentication scheme is adopted with this standard [12].

The communication range performance of a RFID system depends mainly on the choice of frequency, transmitted power from the reader, sensitivity of tag, tag's modulation efficiency, data rate, reader receiver sensitivity, and location of the tag [13]. Based on the frequency, the RFID system can be considered as Low Frequency (LF), High-Frequency (HF), UHF and Microwave (WF) RFID. Nowadays, the UHF RFID is the most used technology because of its far reading distance (up to 10 meters), passive (battery less) tags,

high security, and strong penetrating force features [14].

As shown in Fig. 2, the controller activates the RFID reader to send RF signals. Tags receive, process and send back the requested data through the tag's antenna. The tag responds with an identification code using backscattering of modulated received signal. There is no battery as a source of energy in the passive tag system, and thereby it gets all the energy needed for running from the electromagnetic wave transmitted by the reader. The reader decodes the received signal through its antenna to be processed by the controller.

In most cases, the reader's antenna is placed in an external module as presented in Fig. 2 to achieve long read/write ranges also when a circularly polarized reader antenna is used to eliminate tag orientation sensitivity. According to different configurations and parameters, UHF RFID readers can be designed as fixed or handheld readers.

Handheld readers are used in a large number of applications for its portable, and easy to use in shift data collection. A handheld UHF RFID reader includes embedded computer middleware and application, microwave and antenna designs, radio frequency electronic circuits, wireless communications and signal processing, low-power control and many other technical fields. In this

research, embedded RFID reader is taken into consideration to reduce the overall system cost and complexity.

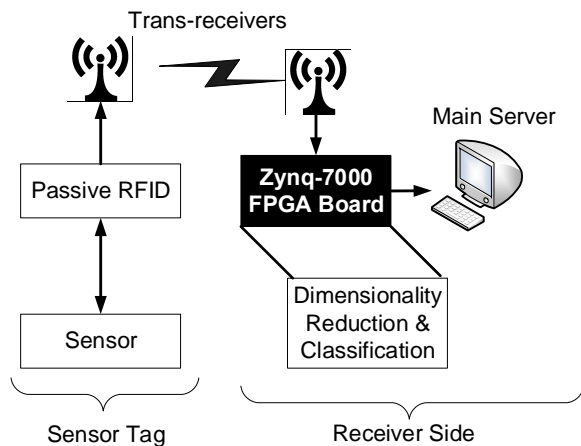


Fig. 2. RFID system architecture diagram.

3.1. Antenna Design

Among the important performance characteristics is the maximum range at which RFID reader can detect the backscattered signal from the tag. Because reader sensitivity is typically high in comparison with a tag, the reading range is defined by the tag response threshold. Communication range is also sensitive to the tag orientation, the material the tag is placed on, and to the propagation environment. The reader antenna should be a circularly polarized antenna, in order to avoid the polarization loss when the orientation of the identified object is changed. The read range r can be calculated using Friis free-space formula as [add a reference]:

$$r = \frac{\lambda}{4\pi} \sqrt{\frac{P_t G_t G_r \tau}{P_{th}}}, \quad (1)$$

where λ is the wavelength, P_t is the power transmitted by the reader, G_t is the gain of the transmitting antenna, G_r is the gain of the receiving tag antenna, P_{th} is the minimum threshold power necessary to provide enough power to the RFID tag chip, and τ is the power transmission coefficient.

3.2. Link Budget

In UHF RFID systems, the forward link depends on the tag sensitivity (P_{tag}), while the return link depends on the reader sensitivity (P_{reader}). The reader can process the tag response data when the tag signal power (P_r), received at the reader, is larger than the reader sensitivity. The reader sensitivity is the minimum power of the received tag signal necessary for successful data processing and is mainly defined by the level of self-jammer [15]. One important characteristic is the needed reader sensitivity to detect

an arbitrary tag at the maximum possible distance. From [15], the needed reader sensitivity must be better or equal to:

$$P_{reader} = \frac{P_{tag}^2 * K}{P_t}, \quad (2)$$

where K is the tag backscatter gain and P_t is the reader output power. The given equation is valid for any propagation environment. Fig. 3 shows the reader sensitivity requested by the tags to read command at their maximum possible range [15]. The backscatter gain is assumed to be -10 dB. The study illustrated in Fig. 3 uses four readers with four levels of output power 30 dBm, 20 dBm, 10 dBm and 0 dBm.

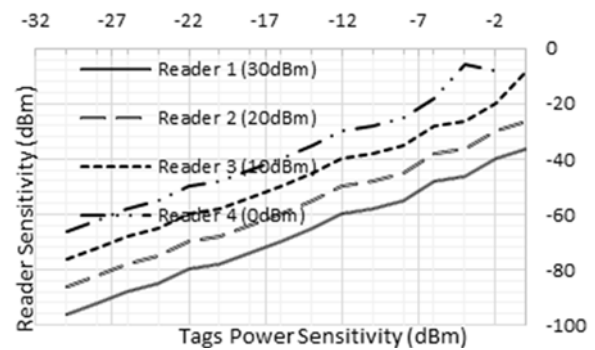


Fig. 3. Reader sensitivity comparison at -10 dB backscatter gain.

3.3. ThingMagic M6e Embedded RFID Reader

To further verify the performance of the proposed UHF tag [16] for both near- and far-field operations, the ThingMagic M6e embedded RFID reader module [17] is studied to be used with a circularly polarized antenna in the free space. This RFID reader module supports the ability to transmit up to 31.5 dBm for the UHF RFID band of 902-928 MHz and can read more than 750 tags/sec. This performance makes M6e the recommended RFID reader for challenging applications such as gas identification and temperature monitoring. The M6e has both serial and USB interfaces to support both board-to-board and board-to-host connectivities.

The maximum tags read range can reach up to 9 meters for an operating temperature from -40 °C to 60 °C.

4. UHF RFID Tags

Fig. 4 shows a simplified block diagram of the RFID tag. It is composed of three main blocks, namely, the analog front-end, the digital baseband core including memory, and the interface to sensors. The energy recovery and power distribution unit rectifies the received RF signals to provide multiple supply voltages for all the other building blocks. A storage

capacitor serves to store energy and supply power to the complete system. Voltage reference and regulator provide stable DC voltages. The power-on-reset (POR) block resets the digital core when the supply voltage reaches a reliable regulated level. A demodulator is implemented to retrieve the baseband data from the carrier frequency. The digital core digitizes the acquired baseband symbols to identify the instructions received from the reader, which consist of reading data from or writing to the implemented one time programmable (OTP) memory. Later, the sensing data stored in the tag's memory can be read out for further processing as necessary. For data transmission the modulator transforms the input impedance of the RFID tags, and thus modulates the backscattered electromagnetic waves, which are further detected and treated by the RFID reader.

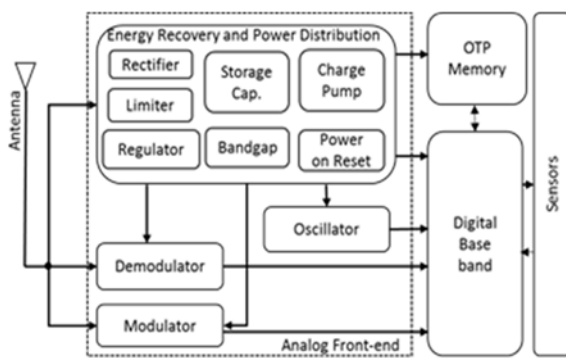


Fig. 4. Block diagram of the proposed UHF passive RFID tag.

4.1 Tags Analog Front-end

The Energy Recovery and Power Distribution Unit (ERPDU) of the RFID tag provides various supply voltages for all building blocks to save the power of the whole system shown in Fig. 4. In addition, the ERPDU generates the bias voltages for the analog modules and a POR signal for the digital core. The rectifier provides the supply for the Band-Gap Reference (BGR), and performs the RF to DC conversion and then the DC output is covered by a limiter which protects the regulator and voltage reference generator from breakdown.

We essentially focus on the power conversion efficiency when designing a rectifier. In this work, we implement diode connected MOS transistor with very low threshold voltage and Metal-Insulator-Metal (MIM) capacitors to improve the conversion efficiency, as Fig. 5 shows. N is the total number of transistor stages. Larger N allows a higher output voltage. Thus, we must select the suitable N to accomplish the optimal value of both the efficiency and output voltage.

Further, the voltage limiter is proposed to avoid the negative impact of high-voltage signals in various blocks. The design is based on a voltage regulator structure using clamping voltage topologies as described in [16]. Voltage regulation employs Low-Drop-Out regulator (LDO) as shown in Fig. 6.

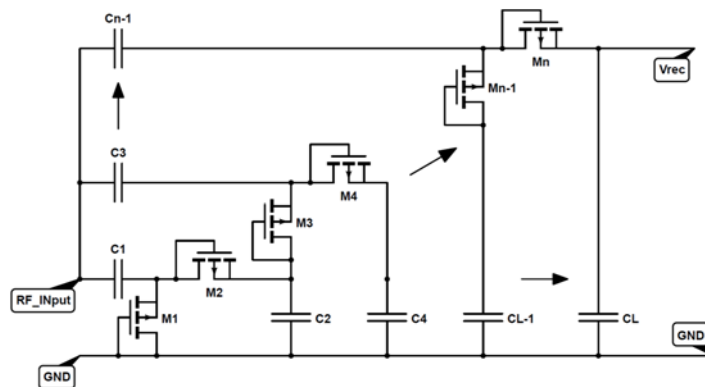


Fig. 5. N-stage rectifier.

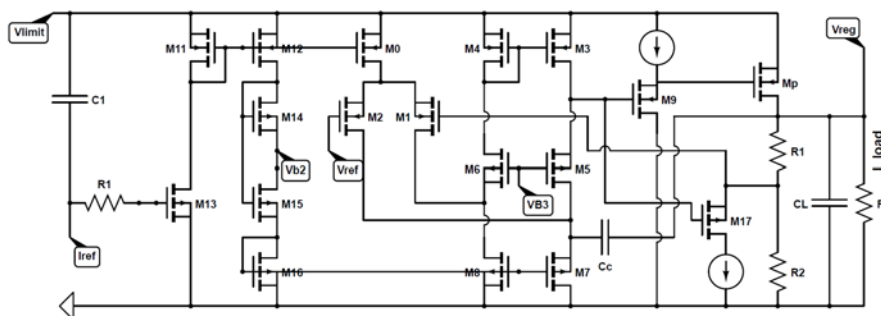


Fig. 6. Low-dropout regulator.

To guarantee LDO stability, we integrated embedded current buffer which is compensated with a feed-forward stage. High voltages used for programming the OTP memory are generated by the charge pump. A storage capacitor is employed to provide both the load current and the reverse leakage current that flow back to the rectifier. When the rectifier charges up the storage capacitors and, through diode-connected transistors, the BGR, regulator, and demodulator. The BGR generates the reference signals for the oscillator as shown in Fig. 4 and the reference voltage for the regulator. Fig. 7 illustrates the implemented bandgap reference optimized for the passive tags.

The demodulator converts the Amplitude Shift Keying (ASK) modulated input signal into digital values. A novel sub-1V demodulator is employed, where its architecture consists of one stage Voltage Multiplier (VM), Low-Pass Filter (LPF), and hysteresis comparator. As shown in Fig. 8, the VM identifies the envelope of the modulated signal. After the signal passes through the VM, the envelope of incoming data flows to the comparator with hysteresis. On the other hand, the modulator presented in Fig. 9 (a) is realized by a MOS transistor M5 which acts as a switch with buffer (M1-M4). By switching on and off this MOS transistor the transponder's input impedance can be modulated. The modulated signal is called backscatter continuous wave. A low-power Voltage Controlled Ring Oscillator (VCRO) is implemented

as a clock generator to avoid the use of a power-hungry one. The generated system clock frequency can vary from 2 to 6 MHz, while theoretically, the minimum clock frequency for robust data decoding is 1.92 MHz in the EPC Gen-2 standard [12]. A low power VCRO capable of functioning as a local oscillator for the tag circuits is achieved by biasing the delay cells to operate in weak inversion region. The design is based on two stage VCRO as shown in Fig. 9(b). The oscillation frequency is fixed by tuning the resistance of transistors M13-M16.

4.2. Digital Baseband Unit

As compared to other non-EPC RFID systems with simple data coding and state management schemes, EPC Gen2 standard features a more robust communication flow with more advanced data encoding, error detection, and anti-collision schemes. To address this challenge, low-power design techniques are employed for the proposed Digital Baseband Unit (DBU) including asynchronous design, clock-gating, low operating frequency, and reuse of registers. Digital section is the baseband processor of the Tag, it performs decoding, CRC checking and calculation, command process, accessing memory, and encoding message back to Reader. Fig. 10 shows the architecture of the digital section inside the passive UHF RFID tag.

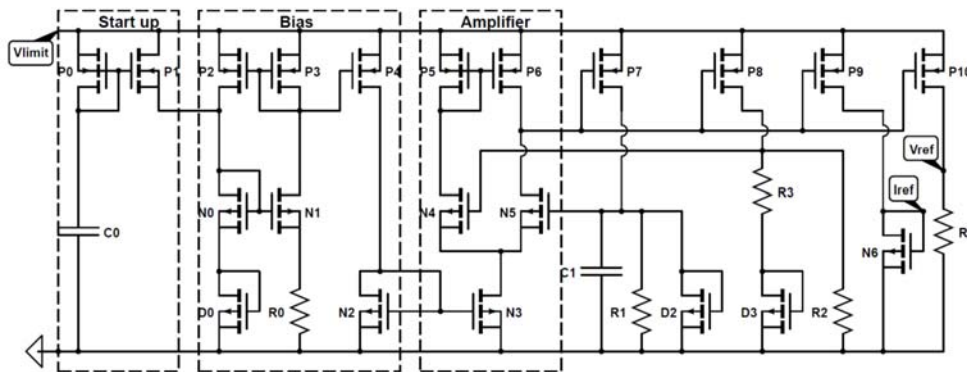


Fig. 7. Bandgap reference design.

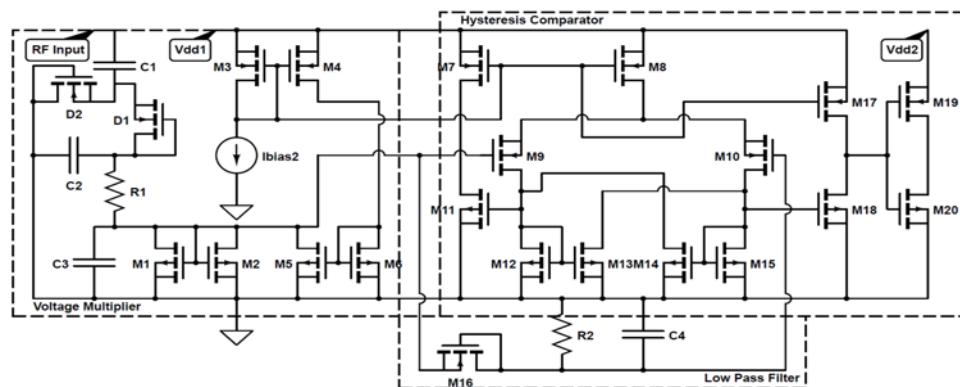


Fig. 8. Demodulator.

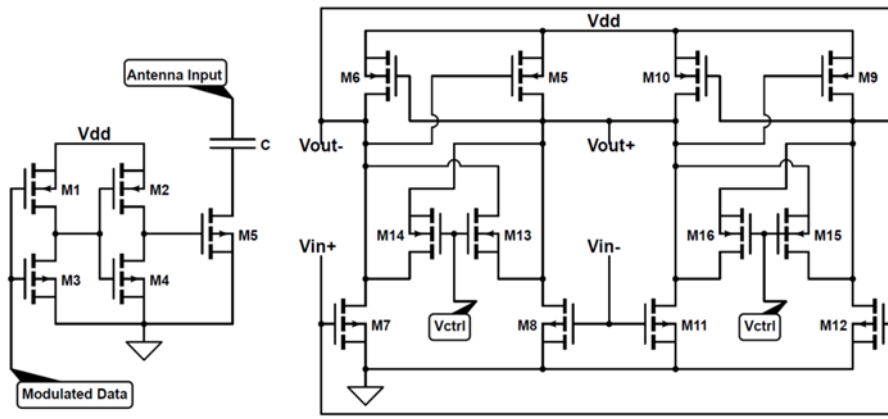


Fig. 9. (a) Modulator, (b) Ring Oscillator.

Our focus was on the reduction of the instantaneous power and how making the power consumption more evenly distributed over the whole operation period. So, the proposed design employs a new architecture of baseband processing of passive UHF RFID Tag, as shown in Fig. 11, which is fully compatible with the EPC Gen2 protocol.

Table 1 shows the division of the employed modules, their driving clock and function are also described. In conventional designs, the Command Processing module always consumes the most power due to its logic complexity, but in our proposed design, Command Processing module only dissipates less than 10 % of total power in average, because of its low operating frequency and closely gated clock. In conventional synchronous architecture, all the sequential circuits dissipate power every clock cycle. However, not all integrated modules are running the required function which leads to dissipate much power. So disable the clock of unnecessary modules can reduce the instantaneous current and power significantly. In addition, a shift-register is usually employed in conventional baseband design to store the decoded data. As EPC Gen2 protocol specifies, in “Select” command, “Length” parameter is 8 bits, allowing “Mask” from 0 to 255 bits in length, which means a huge shift-register is needed to store the “Select”. Meanwhile, in most previous tag designs, the power limitation is in the “receive” state due to data modulation [18].

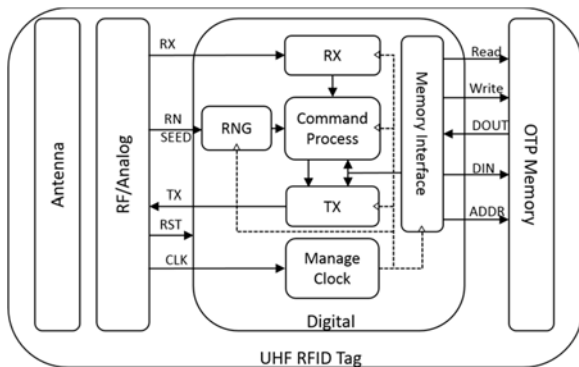


Fig. 10. Block diagram of the proposed low-power digital baseband unit.

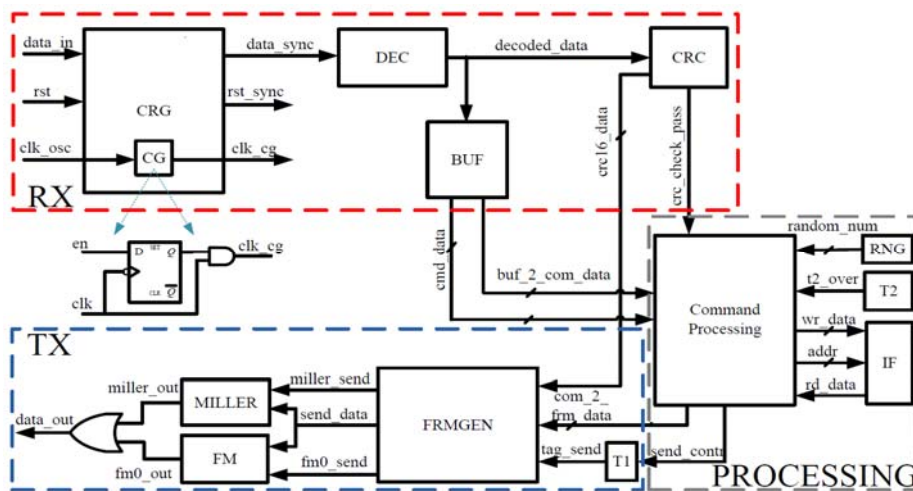


Fig. 11. Architecture of the proposed digital baseband unit.

Thus, the conventional design scheme will lead to high power requirement and large chip size. In our asynchronous design technique, latch bank is used to replace the shift register. From the study in [19], we can consider that latch dissipates much less power (50 % reduced) and smaller area (40 % reduced) than register and is especially suitable for designing a low-cost low-power passive Tag. The Latch is suitable for storing data which have little change once it was loaded.

Table 1. DBU modules, driving clock, and functions.

Module	Clock	Function
CRG	CLK_OSC	Clock/reset generator
DEC	CLK_OSC_DEC	PIE decoder
CRC	CLK_BIT/BLF_CRC	CRC check/calculation
BUF	CLK_BIT_BUF	Command buffer
MD-PROCESS	CLK_BLF_CMD	Command processing
FRMGEN	CLK_BLF_FRMGEN	Reply frame generator
IF	CLK_BLF_IF	Memory interface
RNG	CLK_BLF_RNG	Random number generator
MILLER	CLK_BLF_MILLER	Miller encoder
FM	CLK_BLF_FM	FM0 encoder
T1	CLK_BLF_T1	T1 time control
T2	CLK_BLF_T2	T2 time control

5. Processing Unit

The data received by the RFID receiver is fed to the processing unit for analysis. The possibility of parallel computation in dedicated hardware makes it much faster than the software at run-time. Therefore the processing unit is implemented on heterogeneous reconfigurable Zynq platforms which is having an ARM processor and FPGA chip based on Xilinx 7-series [20]. The reason of selecting the Zynq platform is due to its suitability for hardware/software co-design approach. It is worth noting that the purpose of hardware platform is to process the D_t , whereas the training part is done offline using MATLAB. This is to reduce the hardware overhead caused by the complexity of the feature reduction and classification algorithms. Also, the D_I is used one time for training purpose, so it is more feasible and efficient to do the training offline. Thus, the hardware processing unit is used to perform real-time feature reduction and classification on test data of gases.

5.1. Feature Reduction

The two most common techniques for feature reduction is PCA and LDA both of them have been analyzed in the designed prototype for gas identification so that the best approach can be adopted for final implementation. The aim of feature reduction

is to reduce the feature size without losing useful information. PCA and LDA-based feature reduction algorithms are summarized in Fig. 12.

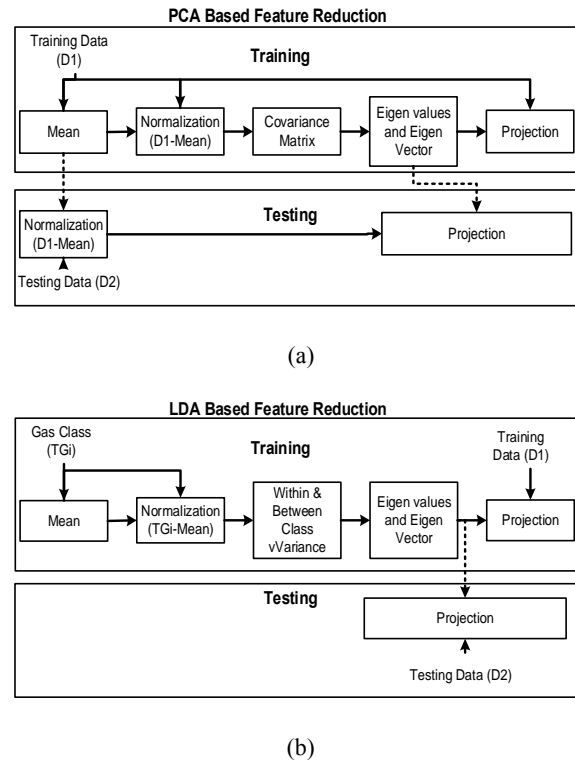


Fig. 12. Feature reduction algorithm based on (a) PCA and (b) LDA.

In case of PCA the Eigenvectors (Ev) and mean values will be computed for training data D_I and then the projection of D_I in the new space is obtained by multiplication of normalized data with the Ev using MATLAB. Whereas, since the testing part requires only Eigen vectors and mean values, as shown in Fig. 12 (a) [21], therefore in case of PCA the computed mean and Ev for D_I is pre-stored in the flash memory of the board and at run-time the hardware will take those values to perform normalization and projection of D_t with lower complexity and faster speed.

In contrast to PCA, LDA is not performed directly on D_I because the goal of LDA is to reduce the inter-class differences and simultaneously increase the differences between classes. Therefore, LDA deals with class boundaries which cannot be identified in D_I . Therefore, D_I is split into classes such that data for each gas is considered as a single class. The training-data obtained at different concentrations of gas are stored as a train-class (T_c), where sub-script c is representing the type of gas. After computing normalization as well as between and within class-differences, the Ev will be computed. The Ev is then forwarded to the projection block which projects the D_I on reducing feature space. It is worth noticing that LDA testing part requires only Eigen vectors as shown in Fig. 12 (b) to project D_t on reducing feature space.

5.2. Classification

A Binary Decision Tree (BDT) classifier is used to identify the gases with and without the feature reduction. The reason of selecting BDT for classification is because of the simplicity and good performance. The tree formation is carried out on DI using MATLAB library function, whereas the decision nodes will be implemented in hardware using successive if-else conditions to classify the gases at run-time from the obtained Dt.

6. Implementation Results

The implementation results for processing unit and RFID module presented in this section. Two different sets of gases have been explored, therefore the implementation result for each set is presented in the following sections.

6.1. Gas Set 1 and Set 2 (GS1 and GS2)

The classification of GS1 has been carried out using BDT and the results has been presented in [22]. The software simulation is carried out using MATLAB whereas the hardware implementation is achieved using Vivado HLS tools [23]. It has been observed that for classification BDT with three principal components can classify 90 % of gases [21] and is therefore 7 % better than using LDA based feature reduction, as shown in Table 2.

However, for hardware implementation LDA based feature reduction requires 50 % less LUTs and 57 % less Flip-Flops (FF) than PCA. Moreover, LDA requires 37.5 % less latency time than PCA, where latency time is the period required to produce the final output, as shown in Table 3.

Table 2. Percent-accuracy results for gas-classification obtained from software simulations.

Gas Set	Properties	LDA (%)	PCA (%)		
			2-PCA (%)	3-PCA (%)	4-PCA (%)
GS1		83	80	90	90
GS2	Steady State (SS)	91	77	87	91

Table 3. Hardware implementation results for gas-classification.

Gas Set	Properties	LDA	PCA (%)		
			2-PCA	3-PCA	4-PCA
GS1	FF	893	1656	2089	2089
	LUT	1937	3024	3925	3925
	Clock Cycles (CC) (Nanoseconds) ns	8.20	8.20	8.20	8.20
	Latency Period (CC)	163	263	261	261
	Input Interval (CC)	164	264	262	262
GS2	FF	1641	1912	2521	2843
	LUT	3406	3968	4882	5227
	Clock Cycles (CC) (Nanoseconds) ns	8.20	8.20	8.20	8.22
	Latency Period (CC)	165	261	261	266
	Input Interval (CC)	166	262	262	267

Furthermore, the BDT obtained with LDA based feature reduction algorithm exhibits only 2 decision nodes along with unity depth, while in case of PCA the BDT have 4-decision nodes with three steps in depth. Therefore, LDA offers simplified decision tree which requires less time for searching and classification of gas than PCA, as shown in Fig. 13.

For GS2, the BDT is shown in Fig. 14, it is observed that for the given data, classification obtained after LDA is equal to the classification obtained using the first four principal components (4-PCA) and is equal to 91 % as shown in Table 2. However, in terms of the hardware overhead LDA requires 73 % less FF than 4-PCA, whereas the required LUT for LDA is also 53 % less than 4-PCA as shown in Table 2.

Similar to GS1, the BDT after LDA based feature

reduction, with only 5 decision nodes, requires less complexity than 4-PCA. Moreover, only 5 tree leaves is required after LDA based feature reduction, whereas 9 tree leaves are required after PCA based feature reduction.

6.2. RFID Module

Fig. 15 shows the details of the adopted low-power clock strategy when Tag receives a Read command. From these figures, we can conclude that the CRG module is dominant in the power dissipation, while the Command Processing module is negligible compared to the total power consumption of the tag since its running time only lasts several clock cycles.

The proposed UHF RFID tag is implemented and simulated in 0.13 μm CMOS process. The circuit is powered up in 60 μs which satisfies the specification of the EPC Gen-2 standard. The design supports carrier frequency within the 902-928 MHz ISM band with forward and return link data rate up to 200 kbps. The frequency of clock is 2.47 MHz at the control voltage of 1.2 V.

Fig. 16 is the post layout results of the ASK demodulation, rectifier and modulation waveforms the minimum input RF signal that can be demodulated is -17 dBm with an input data rate of 40 kb/s. The modulation index of the RF signal is 90%. The modulated signal from the tag is carried on the continuous wave reader signal.

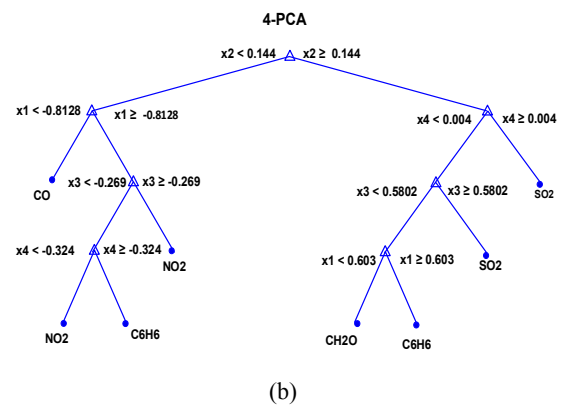
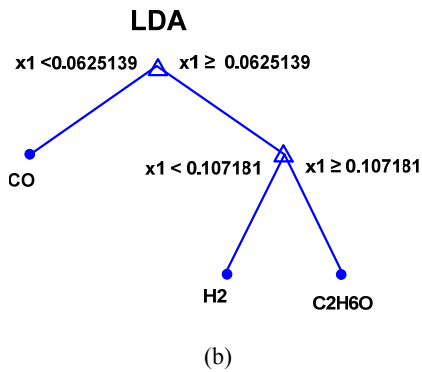
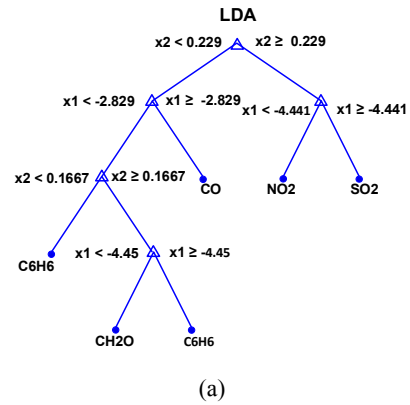
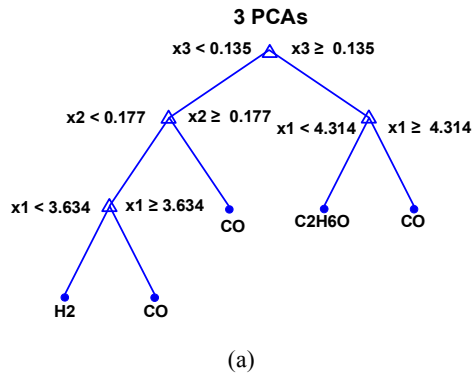


Fig. 13. BDT for GS1: (a) 3-PCA, and (b) LDA.

Fig. 14. BDT for GS2: (a) 4-PCA and (b) LDA.

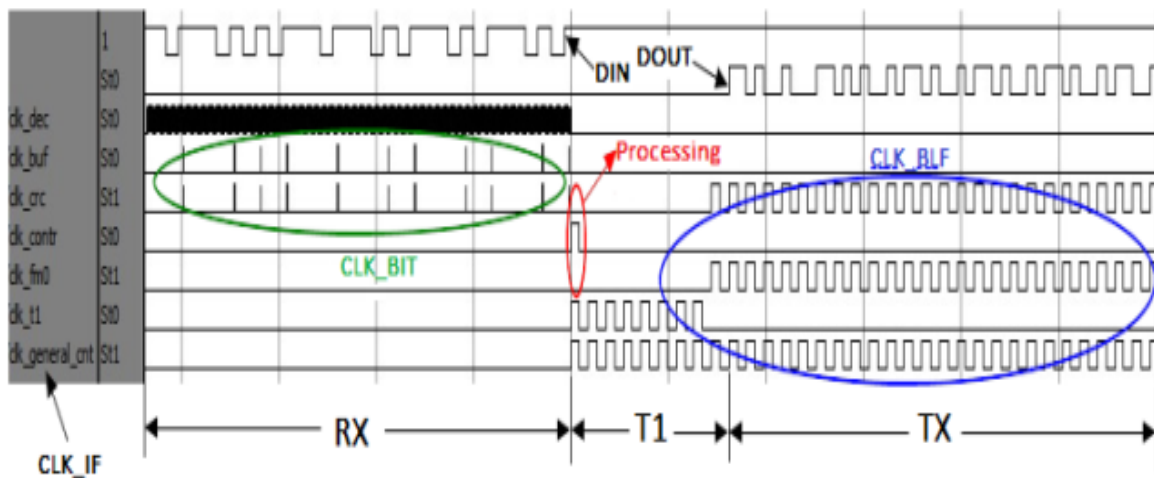


Fig. 15. Low-power clock strategy.

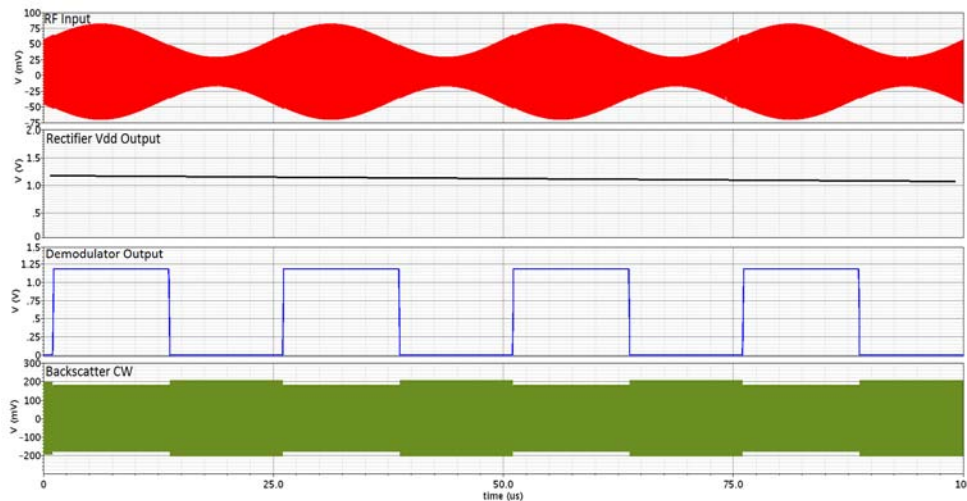


Fig. 16. Simulation results of main blocks of the RF front-end.

7. Conclusions

Since the reader is considered as a key component of the RFID gas application system, therefore a UHF RFID reader is presented with a processing unit implemented on a reconfigurable Zynq platform. The overview of the reader performance characterization is also demonstrated. The RFID system is compliant with the EPC-Gen2 protocol in the 902-928 MHz ISM frequency band. ThingMagic embedded M6e reader shows an advantage over existing readers in the market in term of high integration, low-power dissipation and low cost.

The designed processing unit at the reader is tested using two different sets of gases with PCA and LDA based feature reduction approaches. It is found that for GS1, BDT can classify 90 % of the gases with three principal components which is 7 % more efficient than the identification of gas by BDT using LDA. While in terms of hardware overhead LDA requires 50 % less LUTs than PCA and is 37.5 % more efficient in terms of latency time. Whereas for GS2, classification obtained after LDA is almost equal to the classification obtained using the first four principal components (4-PCA) and is equal to 91 %. However, in terms of the hardware overhead LDA requires 73 % less FF than 4-PCA, whereas the required LUT for LDA is also 53 % less than 4-PCA.

The presented work is part of an ongoing project in which a low-power multi-sensing gas identification platform is need to be developed for gas identification based on an array of tin-oxide gas sensors. Therefore the system will be tested on real conditions after the completion of the integration process.

Acknowledgements

This paper was made possible by National Priorities Research Program (NPRP) grant No. 5 – 080 – 2 – 028 from the Qatar National Research Fund (a member of Qatar Foundation). The

statements made herein are solely the responsibility of the authors.

References

- [1]. N. Yamazoe, N. Miura, Environmental gas sensing, *Sensors and Actuators B: Chemical*, Vol. 20, No. 2-3, 1994, pp. 95-102.
- [2]. S. Labreche, S. Bazzo, S. Cade, E. Chanie, Shelf life determination by electronic nose: application to milk, *Sensors and Actuators B: Chemical*, Vol. 106, No. 1, 2005, pp. 199-206.
- [3]. S. Dragonieri, *et al.* An electronic nose in the discrimination of patients with asthma and controls, *Journal of Allergy and Clinical Immunology*, Vol. 120, No. 4, 2007, pp. 856-862.
- [4]. F. Röck, N. Barsan, U. Weimar, Electronic nose: current status and future trends, *Chemical Reviews*, Vol. 108, No. 2, 2008, pp. 705-725.
- [5]. M. Shi, A. Bermak, S. B. Belhouari, P.C. Chan, Gas identification based on committee machine for microelectronic gas sensor, *IEEE Transactions on Instrumentation and Measurement*, Vol. 55, No. 5, 2006, pp. 1786-1793.
- [6]. B. Guo, A. Bermak, P.C. Chan, G.Z. Yan, An Integrated Surface Micromachined Convex Microhotplate Structure For Tin Oxide Gas Sensor Array, *IEEE Sensors Journal*, Vol. 7, No. 12, 2007, pp. 1720-1726.
- [7]. E. Llobet, *et al.*, Multicomponent gas mixture analysis using a single tin oxide sensor and dynamic pattern recognition, *IEEE Sensors Journal*, Vol. 1, No. 3, 2001, pp. 207-213.
- [8]. L. Yang, R. Zhang, D. Staiculescu, C. P. Wong, M. M. Tentzeris, A novel conformal RFID-enabled module utilizing inkjet-printed antennas and carbon nanotubes for gas-detection applications, *IEEE Antennas and Wireless Propagation Letters*, Vol. 8, 2009, pp. 653-656.
- [9]. M. Brandl, *et al.*, A low-cost wireless sensor system and its application in dental retainers, *IEEE Sensors Journal*, Vol. 9, No. 3, 2009, pp. 255-262.
- [10]. S. Mohamad, F. Tang, A. Amira, A. Bermak, M. Benammar, A Low Power Oscillator Based Temperature Sensor for RFID Applications, in

- Proceedings of the 5th Asia Symposium on Quality Electronic Design (ASQED)*, 2013, pp. 50-54.
- [11]. R. Weinstein, RFID: A Technical Overview and its Application to the Enterprise, *IT Professional*, Vol. 7, No. 3, 2005, pp. 27-33.
- [12]. EPCglobal Inc., EPC Radio-Frequency Identity Protocols Class-1 Generation-2 UHF RFID Protocol for Communications at 860 MHz-960 MHz Version 1.0.9, *EPC Global Standards*, 2005.
- [13]. K. Finkensteller, RFID Handbook, *John Wiley & Sons*, New York, 2003.
- [14]. A. S. Ahson, M. Ilyas, RFID Handbook: Applications, Technology, Security and Privacy, *CRC Press*, 2008.
- [15]. P. Nikitin, K. V. S. Rao, S. Lam, UHF RFID tag characterization: overview and state-of-the-art, in *Proceedings of the 34th Annual Meeting and Symposium on Antenna Measurement Techniques Association Symposium (AMTA)*, 2012, pp. 289-294.
- [16]. M. Zgaren, M. Sawan, A Front end-EPC Gen-2 Passive UHF RFID Transponder for Embedded Gas Sensor, in *Proceedings of the 4th International Gas Processing Symposium*, 2014, pp. 223-231.
- [17]. 'M6e High-Performance 4-Port UHF RFID Module', http://www.dpie.com/manuals/rfid/M6eHardwareGuide_Sept13.pdf, v 1.13.1, accessed May 12, 2015.
- [18]. Y. Ling, *et al.*, System Level Power Optimizations For EPC RFID Tags to Improve Sensitivity Using Load Power Shaping and Operation Scheduling, in *Proceedings of the IEEE International Symposium on Circuits and Systems (ISCAS)*, 2010, pp. 3012-3015.
- [19]. D. Wei, C. Zhang, Y. Cui, H. Chen, Z. Wang, Design of a low-cost low-power baseband-processor for UHF RFID tag with asynchronous design technique, in *Proceedings of the IEEE ISCAS*, May 2012, pp. 2789-2792.
- [20]. Inc Xilinx. Zynq-7000 All Prog. SoC: Tech. Reference Manual, http://www.xilinx.com/support/documentation/user_guides/ug585-Zynq-7000-TRM.pdf, UG585, v1.8.1, accessed Feb. 20, 2015.
- [21]. A. Ait Si Ali, A. Amira, F. Bensaali, M. Benammar, Hardware PCA for Gas Identification Systems Using High Level Synthesis on the Zynq SoC, in *Proceedings of the IEEE 20th International Conference on Electronics, Circuits, and Systems (ICECS)*, 2013, pp. 707-710.
- [22]. M. A. Akbar, A. Ait Si Ali, A. Amira, F. Bensaali, M. Benammar, M. Zgaren, M. Sawan, A. Bermak, Receiver Design of Passive UHF RFID Sensor Platform for Gas Identification, in *Proceedings of the 6th International Conference on Sensor Device and Technologies (SENSORDEVICES' 2015)*, Venice, Italy, 23-28 August 2015, pp. 164-169.
- [23]. 'Inc Xilinx Vivado Design Suite User Guide: Embedded Processor H/W Design', http://www.xilinx.com/support/documentation/sw_manuals/xilinx2013_3/ug898-vivado-embedded-design.pdf, UG898, v2014.3, accessed March 9, 2015

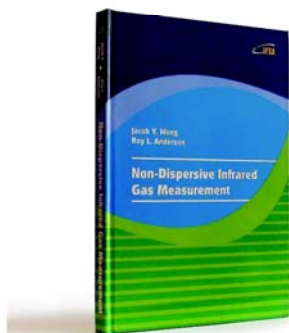
2015 Copyright ©, International Frequency Sensor Association (IFSA) Publishing, S. L. All rights reserved. (<http://www.sensorsportal.com>)



International Frequency Sensor Association (IFSA) Publishing

Jacob Y. Wong, Roy L. Anderson

Non-Dispersive Infrared Gas Measurement



Formats: printable pdf (Acrobat) and print (hardcover), 120 pages

ISBN: 978-84-615-9732-1,
e-ISBN: 978-84-615-9512-9

Written by experts in the field, the *Non-Dispersive Infrared Gas Measurement* begins with a brief survey of various gas measurement techniques and continues with fundamental aspects and cutting-edge progress in NDIR gas sensors in their historical development.

- It addresses various fields, including:
- Interactive and non-interactive gas sensors
- Non-dispersive infrared gas sensors' components
- Single- and Double beam designs
- Historical background and today's of NDIR gas measurements

Providing sufficient background information and details, the book *Non-Dispersive Infrared Gas Measurement* is an excellent resource for advanced level undergraduate and graduate students as well as researchers, instrumentation engineers, applied physicists, chemists, material scientists in gas, chemical, biological, and medical sensors to have a comprehensive understanding of the development of non-dispersive infrared gas sensors and the trends for the future investigation.

http://sensorsportal.com/HTML/BOOKSTORE/NDIR_Gas_Measurement.htm